Biomaterials 35 (2014) 6278–6286

Contents lists available at ScienceDirect

Biomaterials

journal homepage: www.elsevier.com/locate/biomaterials

Sustained localized presentation of RNA interfering molecules from *in situ* forming hydrogels to guide stem cell osteogenic differentiation

Minh K. Nguyen [a,1], Oju Jeon [a,1], Melissa D. Krebs [a,2], Daniel Schapira [a], Eben Alsberg [a,b,c,*]

[a] Department of Biomedical Engineering, Case Western Reserve University, 10900 Euclid Avenue, Cleveland, OH 44016, USA
[b] Department of Orthopaedic Surgery, Case Western Reserve University, 10900 Euclid Avenue, Cleveland, OH 44016, USA
[c] National Center for Regenerative Medicine, Division of General Medical Sciences, Case Western Reserve University, Cleveland, OH, USA

ARTICLE INFO

Article history:
Received 4 March 2014
Accepted 13 April 2014
Available online 13 May 2014

Keywords:
Biomaterials
Mesenchymal stem cells
Tissue engineering
Gene delivery
Bone regeneration

ABSTRACT

To date, RNA interfering molecules have been used to differentiate stem cells on two-dimensional (2D) substrates that do not mimic three-dimensional (3D) microenvironments in the body. Here, *in situ* forming poly(ethylene glycol) (PEG) hydrogels were engineered for controlled, localized and sustained delivery of RNA interfering molecules to differentiate stem cells encapsulated within the 3D polymer network. RNA interfering molecules were released from the hydrogels in a sustained and controlled manner over the course of 3–6 weeks, and exhibited high bioactivity. Importantly, it was demonstrated that the delivery of siRNA and/or miRNA from the hydrogel constructs enhanced the osteogenic differentiation of encapsulated stem cells. Prolonged delivery of siRNA and/or miRNA from this polymeric scaffold permitted extended regulation of cell behavior, unlike traditional siRNA experiments performed *in vitro*. This approach presents a powerful new methodology for controlling cell fate, and is promising for multiple applications in tissue engineering and regenerative medicine.

1. Introduction

Stem cells are an attractive cell source for tissue engineering and regenerative medicine because they exhibit the capacity to self-renew without loss of their multipotency and when presented with specific signals can be driven to differentiate down multiple lineages [1]. Mesenchymal stem cells (MSCs) isolated from, for example, bone marrow, fat and muscle, are a potentially valuable cell source for the engineering of damaged or lost connective tissues due to their ability to differentiate into the cells that ultimately generate these tissues, such as adipocytes, chondrocytes, myoblasts and osteoblasts, in the presence of defined environmental factors [2]. Small interfering RNA (siRNA) can suppress gene expression post-transcriptionally and is a powerful tool for guiding cell behaviors in tissue regeneration applications [3–5]. For example, the protein noggin is an antagonist to the activity of bone morphogenetic proteins (BMP)-2, -4, -5, -6 and -7, which are members of the transforming growth factor superfamily, by binding to them and in turn preventing them from binding to their respective receptors [6,7]. Overexpression of noggin can impair osteogenic differentiation and reduce bone formation in a transgenic mouse model [8,9]. Suppression of noggin gene expression can augment osteogenic differentiation in MC3T3 preosteoblasts, primary mouse calvarial osteoblasts [10], and human adipose-derived stem cells (hADSCs) [5]. More recently, microRNAs (miRNAs), which are also short and non-coding RNA molecules, have similarly been used to guide human bone marrow derived MSC (hMSC) fate upon transfection [11,12]. However, RNA-induced differentiation of MSCs is currently performed on cells cultured on traditional 2D substrates like tissue culture plastic, which do not provide important 3D environmental cues present in natural tissues [3,4,13].

siRNA and miRNA have been delivered using nano- or microparticles; however, these particles rapidly clear from desired sites upon injection *in vivo* due to their small size, which limits their capacity to locally affect cells for an extended period of time [14,15]. In addition, nanofibrous scaffolds [16–18], solid porous scaffolds [19], and hydrogels [15,20–24] have been developed to release siRNA locally to surrounding cells. The nanofibrous and porous scaffolds that have been used lack the capacity for cell encapsulation. In contrast, hydrogels, highly hydrated, 3D hydrophilic polymeric networks, have been extremely attractive for tissue engineering applications for a variety of reasons, including their

* Corresponding author. Department of Biomedical Engineering, Case Western Reserve University, 10900 Euclid Avenue, Cleveland, OH 44016, USA. Tel.: +1 216 368 6425; fax: +1 216 368 4969.
E-mail addresses: eben.alsberg@case.edu, exa46@case.edu (E. Alsberg).
[1] These authors equally contributed to this work.
[2] Current address: Chemical and Biological Engineering Department, Colorado School of Mines, 1500 Illinois Street, Golden, CO 80401, USA.

http://dx.doi.org/10.1016/j.biomaterials.2014.04.048
0142-9612/

compositional and structural similarities to natural extracellular matrix (ECM), their injectability and capacity to gel *in vitro* to take the shape of defects, and the capacity to encapsulate cells within them with high viability and engineer them to locally deliver a variety of bioactive factors in a controlled manner to transplanted or host cells [25–27]. Chitosan [20] and polyphosphazene [21] hydrogels have been used to exogenously supply siRNA to cancer cells to suppress their growth, and we have utilized alginate and collagen [15] hydrogels to locally deliver siRNA to both encapsulated and surrounding cells to knockdown specific protein expression. Recently, functionalized, photocrosslinkable dextran hydrogels were engineered permitting tailorable, sustained siRNA release which offers control over the duration of gene knockdown in target cells [24]. However, to date there have not been any reports on biopolymer scaffolds capable of delivering siRNA to encapsulated stem cells to control their differentiation.

Here, hydrogel scaffolds are used for the controlled, localized and sustained presentation of RNA interfering molecules to guide the differentiation of encapsulated MSCs for tissue regeneration applications. *In situ* forming poly(ethylene glycol) (PEG) hydrogels that provide a platform for controlled, tunable and local release of siRNA and miRNA were engineered to induce osteogenic differentiation of incorporated hMSCs. Importantly, the hydrogels form by simple mixing of two macromer components at physiological conditions without the need of photoinitiators, chemicals or UV exposure that may be harmful to incorporated cells or bioactive factors.

In the field of bone tissue engineering there have been significant research efforts toward developing 3D polymeric scaffolds for the delivery of osteogenic growth factors (e.g., BMP-2) [28–30] or plasmid DNA encoding for these factors [31–33] to upregulate cell expression of osteogenic signals. However, recombinant growth factors can require supraphysiological doses to have an effect, be expensive, be hard to maintain at a constant concentration, and easily affect non-target tissues [34]. Plasmid DNA suffers from challenges such as its import to the cell nucleus, potential integration into the host genome and possible insertional mutagenesis [35,36]. The work presented here is a fundamental shift in approach. Down-regulation of gene expression via siRNA and/or miRNA may be an effective alternative tool to drive osteogenesis. While these studies have previously been difficult to perform due to the transient effect of bolus treatment, a controlled, sustained siRNA/miRNA delivery system that permits the encapsulation of cells, such as that contained herein, permits examination of this approach.

2. Materials and methods

2.1. Synthesis of 8-arm-peg-MAES

Catalyst 4-(dimethylamino)pyridinium 4-toluenesulfonate (DPTS) was synthesized by adding 10 ml of *p*-toluenesulfonic acid monohydrate (PTSA, Sigma, St. Louis, MO) solution (0.38 g/ml) in tetrahydrofuran (THF, Fisher Scientific, Pittsburgh, PA) to 30 ml of saturated DMAP (Sigma) solution (0.081 g/ml) in THF under stirring. DPTS was then precipitated, filtered, washed with THF, and dried under vacuum. 8-arm-PEG-OH (5 g, 10,000 g/mol, JenKem Technology USA, Allen, TX) was dissolved with 100 ml methylene chloride (MC, Fisher Scientific) in a dry 250 ml round bottom flask equipped with a stir bar. After complete dissolution of the PEG, DCC (2.47 g, Sigma), mono(2-acryloyloxyethyl) succinate (MAES, TCI America, Portland, OR) and DPTS (0.38) were added and the reaction occurred at room temperature for 1 d. To collect the 8-arm PEG-MAES, the reaction solution was filtered, concentrated under vacuum, and precipitated in a 2:1 mixture of ether and hexane. The polymer was further purified via dialysis (3500 Da cutoff membrane) in deionized water (diH_2O) for 3 days at 4 °C and then frozen and lyophilized until dry. The polymer was characterized with ^1H NMR in D_2O.

2.2. Synthesis of 8-arm-peg-A

8-arm-PEG-OH (5 g) was dissolved in 45 ml toluene (Fisher Scientific), and TEA (1.7 ml, Sigma) and acryloyl chloride (AC, Sigma) (1.06 ml) was added dropwise to the PEG solution at 0 °C. The reaction was performed at 40 °C for 16 h. The polymer was collected by concentrating the solvent and precipitating in a 2:1 mixture of ether and hexane. To further purify, the polymer was hydrated with diH_2O and dialyzed against diH_2O at 4 °C using 3500 Da cutoff membrane for 3 days. The polymer solution was then frozen and lyophilized until dry. The conjugation was confirmed with ^1H NMR.

2.3. Hydrogel formation and gelation time

Hydrogels were fabricated by mixing 8-arm-PEG-MAES or 8-arm-PEG-A and 8-arm-PEG-SH (10,000 g/mol, JenKem Technology USA) solutions in phosphate buffered saline (PBS, pH 7.4, Fisher Scientific) with a 1:1 stoichiometry ratio of acrylate and thiol groups to obtain a final concentration of 15 %w/v. After vortexing for 10 s, the macromer solutions (100 μl) were immediately placed into a 15 ml conical tube and allowed to gel at room temperature. Hydrogels formed within 2 min, but they were incubated for a further 2 h to achieve maximum gelation.

Gelation time of the hydrogels was determined via the visual tube inversion method [37] at room temperature. Specifically, each macromer solution (100 μl) was added to a microcentrifuge tube and vortexed for 10 s, and gelation time was then monitored. The gelation time was determined as the point when the solution stopped flowing in the inverted tube ($N = 3$).

2.4. Swelling and degradation experiments

The swelling ratios of the PEG hydrogels were determined by measuring their dry and wet weights at different time points. The initial dry weights (W_{di}) of lyophilized gels were measured, and each dry gel was then placed into a 15 ml conical tube containing 10 ml PBS at pH 7.4 and incubated at 37 °C. The media was changed every 3 days. At predetermined time points, the samples were collected and rinsed with diH_2O, and their swollen weights (W_s) were measured. The swelling ratio (Q) was determined by $Q = W_s/W_{di}$. To determine their mass loss at each time point, the same procedure as the swelling experiment was performed, but instead of measuring W_s the samples were rinsed with diH_2O, frozen and lyophilized to obtain dry weights (W_d). The percentage mass loss of the gels was determined by $(W_{di}-W_d) \times 100/W_{di}$. Three hydrogels per condition ($N = 3$) were used for each condition at each time point.

2.5. Rheology

Rheological properties of the *in situ* formed hydrogels were measured using a Haake Mars III Rotational Rheometer (Thermo Fisher Scientific Inc., Waltham, MA). Hydrogels were prepared by mixing the precursor solutions and pipetting them between two-glass plates separated by two 0.75 mm spacers. They were allowed to form for 10 min, and the hydrogel discs were then punched out using a 0.8 cm biopsy punch. To perform the rheology, each gel disc was placed between two stainless steel parallel plates (0.8 cm in diameter). Storage (G') and loss (G'') moduli of each hydrogel were measured by performing a dynamic frequency sweep test with a constant maximum shear strain amplitude (0.1%) over a frequency range of 0.1–10 Hz at 37 °C. $N = 3$ per condition.

2.6. siRNA release

siRNA fluorescently tagged with fluorescein isothiocyanate (FITC), Green cyclophilin B control siRNA (Thermo Scientific Dharmacon, Lafayette, CO), was used to examine its release kinetics from the PEG hydrogels. siRNA was complexed with branched PEI (25,000 g/mol, Sigma) in nuclease free PBS pH 7.4 (Life Technologies, Grand Island, NY) with an N/P ratio of 10 to form polyplexes that were then encapsulated within the hydrogels prepared as described above. 4 μg of siRNA was used for each 100 μl hydrogel. Each hydrogel loaded with siRNA/PEI nanocomplexes was formed in a 15 ml conical tube and then 1 ml of PBS was added. The release was carried out at 37 °C and the PBS was removed and replaced with 1 ml of fresh PBS at each time point. Standard curves were prepared using siRNA/PEI nanocomplexes as described above. The siRNA samples were measured in 1 N NaOH solutions, to dissociate the complexes, using a plate reader (fmax, Molecular Devices, Sunnyvale, CA) set at excitation 485/emission 538 ($N = 3$).

2.7. Bioactivity evaluation

To determine released siRNA bioactivity, siRNA targeting GFP (siGFP) and luciferase (siLuc) (Thermo Scientific Dharmacon) were complexed with PEI as described above and the siRNA/PEI complexes were released from the hydrogels. The siRNA/PEI complexes were released in PBS as described above, and releasates

Table 1
Sequences of RNA interfering molecules.

RNA name	Sense sequence
siGFP	5′-GCA AGC UGA CCC UGA AGU UC-3′
siLuc	5′-GAU UAU GUC CGG UUA UGU AUU-3′
siNoggin	5′-AAC ACU UAC ACU CGG AAA UGA UGG G-3′
miRNA-20a	5′-UAA AGU GCU UAU AGU GCA GGU AG-3′
Negative control	5′-UUC UCC GAA CGU GUC ACG UTT-3′

Table 2
Primer sequences used for qRT-PCR.

Gene	Direction	Primer sequence
GAPDH	Forward	GGGGCTGGCATTGCCCTCAA
	Reverse	GGCTGGTGGTCCAGGGGTCT
Noggin	Forward	CTCTAGCGAGGGTTTTCAAT
	Reverse	GTGCATTACAGGAACCAGAA
ALP	Forward	GACAAGAAGCCCTTCACTGC
	Reverse	AGACTGCGCCTGGTAGTTGT
Runx2	Forward	ACAGAACCACAAGTGCGGTGCAA
	Reverse	TGGCTGGTAGTGACCTGCGGA
BSP	Forward	ACCCTAACCCTGGAGAGCCCCT
	Reverse	TCGCCTTGAGATATCGGGGGCA
PPAR-γ	Forward	GGCCTCGAGGACAACGGAGA
	Reverse	AGTTGGTGGGCCAGAATGGCA

were collected every 5 days and replaced with fresh PBS. The last releasates collected when the hydrogels completely degraded were used for bioactivity evaluation. One day before transfection, destabilized GFP (deGFP)-expressing HEK293 cells (passage 27; a generous gift from Piruz Nahreini, PhD., University of Colorado Health Sciences Center) were plated onto 24-well plates (Fisher Scientific) at a density of 100,000 cells per well and cultured for 24 h in a humidified incubator at 37 °C and 5% CO_2. On the day of transfection, the HEK293 cells were treated with the siRNA/PEI release samples (0.26 μg siRNA). The complexes were incubated with the cells for 6 h, and then the media was replaced with Dulbecco's Modified Eagle Medium High Glucose (DMEM-HG, HyClone, Logan, UT) containing 10% fetal bovine serum characterized (FBS, HyClone). After two additional days of culture, the cells were harvested and suspended in PBS for GFP knockdown quantification using a flow cytometer (EPICS XLMCL, Beckman Coulter, Fullerton, CA). Freshly prepared siLuc/PEI and released siLuc/PEI complexes were used as negative controls. Bioactivity of the released siGFP/PEI complexes was compared to that of freshly prepared siGFP/PEI complexes. The results were normalized to cells without siRNA treatment ($N = 3$).

2.8. Osteogenic differentiation of hMSCs encapsulated in hydrogels

hMSCs were isolated from the posterior iliac crest of healthy donors under a protocol approved by the University Hospitals of Cleveland Institutional Review Board and processed as previously described [38]. Briefly, the aspirates were washed with growth medium comprised of Low Glucose Dulbecco's Modified Eagle's Medium (DMEM-LG, Sigma) with 10% prescreened FBS [39]. Mononuclear cells were isolated by centrifugation in a Percol (Sigma) density gradient and the isolated cells were plated at 1.8×10^5 cells/cm^2 in growth medium. Medium was changed every 3 days and after 14 days of culture the cells were passaged at a density of 5×10^3 cells/cm^2. hMSCs (passage 3) were suspended in hydrogel solutions containing siNoggin (Insight Genomics, Falls Church, VA), miRNA-20a (Insight Genomics), equal amounts of siNoggin and miRNA-20a, or non-targeting negative control siRNA (Insight Genomics) (40 μg/ml gel) complexed with PEI at a density of 5×10^6 cells/ml. The siRNA and the miRNA-20a sequences are listed in Table 1. The macromer solutions in DMEM-LG were pipetted into

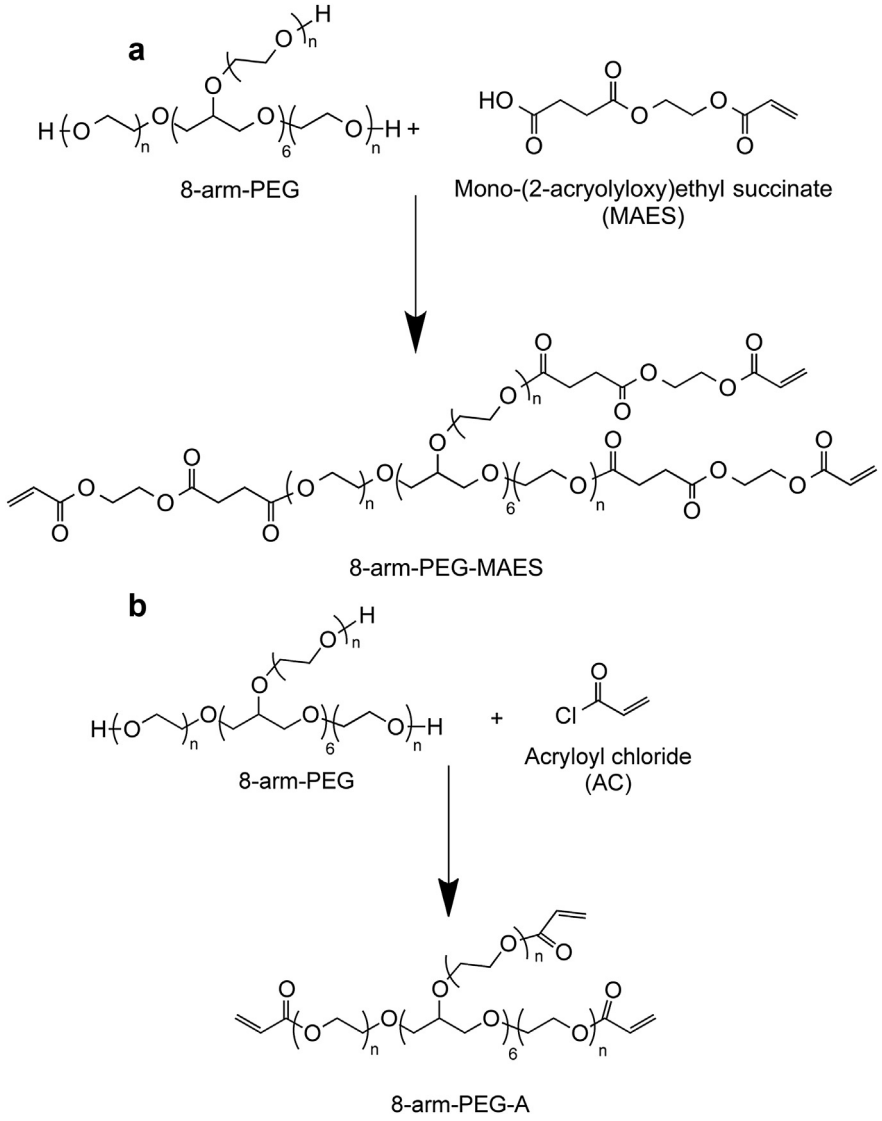

Fig. 1. Synthesis of (a) 8-arm-PEG-MAES and (b) 8-arm-PEG-A.

microcentrifuge tubes and vortexed for 10 s, and the hydrogels (100 μl) were formed at room temperature. Then each gel was transferred into individual wells of 24-well plates containing 1 ml osteogenic media (10 mM β-glycerophosphate (CalBiochem, Billerica, MA), 50 μM ascorbic acid (Wako USA, Richmond, VA), 100 nM dexamethasone (MP Biomedicals, Solon, OH) and 100 ng/ml BMP-2 (Department of Developmental Biology, University of Würzburg, Germany). The osteogenic media was changed two times a week. At predetermined time points, each hydrogel-cell construct was removed from the 24-well plates, put in 1 ml alkaline phosphatase (ALP) lysis buffer [1 mM $MgCl_2$ (Sigma), 20 μM $ZnCl_2$ (Sigma), 0.1% octyl-beta-glucopyranoside (Sigma)] and homogenized at 35,000 rpm for 60 s using a TH homogenizer (Omni International, Marietta, GA). The homogenized solutions were centrifuged at 500 g with a Sorvall Legend RT Plus Centrifuge (Thermo Fisher Scientific). The supernatants were collected for ALP, calcium and DNA analysis ($N = 3$).

For ALP measurement, the supernatant (100 μl) was treated with p-nitrophenylphosphate (pNPP, 100 μl, Sigma) substrate, and then 0.1 N NaOH (50 μl) was added to stop the reaction. The absorbance was measured at 405 nm using a plate reader (VersaMax, Molecular Devices, Sunnyvale, CA). Calcium content of the constructs was quantified using a calcium assay kit (Pointe Scientific, Canton, MI) according to the company's instructions. The supernatant (4 μl) was mixed with a color and buffer reagent mixture (250 μl), and the absorbance was read at 570 nm on the plate reader. DNA was measured using a Picogreen assay kit (Invitrogen) on a plate reader (fmax, Molecular Devices) set at excitation 485/emission 538. All of the ALP and calcium measurements were normalized to DNA content. Calcium deposition in the bulk gels was stained with Alizarin red (Sigma). Cell-hydrogel constructs were fixed with 4% paraformaldehyde overnight and then stained with 2% Alizarin red solution (pH 4.2) at room temperature for 5 min. The stained cell-hydrogel constructs were imaged using an iPhone 5 digital camera (Apple, Cupertino, CA) after washing the cell-hydrogel constructs three times for 30 min with deionized ultrapure water. To further investigate the mineralization of cell-hydrogel constructs, fixed constructs were embedded in paraffin, sectioned at a thickness of 10 μm, and examined with Alizarin red staining.

2.9. Cytotoxicity

Viability of hMSCs encapsulated with siRNA and/or miRNA in the hydrogels during the osteogenic differentiation study was assessed with a live/dead assay comprised of fluorescein diacetate (FDA, Sigma) and ethidium bromide (EB, Fisher Scientific). The staining solution was prepared by mixing 1 ml of FDA solution (1.5 mg/ml in dimethyl sulfoxide, Sigma) and 0.5 ml of EB solution (1 mg/ml in PBS) with 0.3 ml of PBS (pH 8). After one day of culture, 20 μl of live/dead staining solution was added into each well containing 1 ml osteogenic media, and the hMSC/hydrogel constructs were imaged with a fluorescence microscope (ECLIPSE TE 300; Nikon, Tokyo, Japan) equipped with a digital camera (Retiga-SRV; Qimaging, Burnaby, BC, Canada) after 3–5 min incubation at room temperature.

2.10. RNA Isolation and real-time quantitative reverse transcription-polymerase chain reaction (qRT-PCR)

RNA was isolated from encapsulated hMSCs using TRI reagent (Sigma) according to the manufacturer's instructions. Specifically, the cell-hydrogel constructs were put in 1 ml TRI reagent and homogenized at 35,000 rpm for 60 s with a TH homogenizer. After centrifuging the homogenized solutions at 12,000 g for 15 min using a microcentrifuge (accuSpin Micro 17R, Fisher Scientific), the supernatants were further processed for RNA isolated followed by cDNA synthesis. cDNA was prepared using a cDNA synthesis kit (PrimeScript™ RT Reagent Kit with gDNA Eraser, Takara Bio, Mountain View, CA) according to the manufacturer's instruction, and then used for qRT-PCR analysis with SYBR® Premix Ex Taq™ II (Tli RNase H Plus) kit (Takara Bio). The primer sequences used for qRT-PCR reactions, which were performed on an ABI 7500 Real-Time PCR instrument (Applied Biosystems), are listed in Table 2. The relative gene expression levels of noggin ($N = 5$), Runx2 ($N = 6$), BSP ($N = 6$) and PPAR-γ ($N = 3$–6) were normalized to the control group at each time point.

2.11. Statistical analysis

All values represent mean ± standard deviation. Statistical significance was performed with one-way analysis of variance (ANOVA) with Tukey significant difference post hoc test using InStat software (GraphPad Software, La Jolla, CA). $p < 0.05$ was considered statistically significant.

3. Results and discussion

3.1. Synthesis, characterization, hydrogel formation and gelation time

8-arm-PEG-MAES was synthesized via the esterification reaction of the hydroxyl groups of 8-arm-PEG and the carboxylic acid of MAES in the presence of DPTS as a catalyst (Fig. 1a). 8-arm-PEG-A was prepared by the reaction of the hydroxyl groups of PEG with AC (Fig. 1b), as previously reported [40,41]. The ^{1}H NMR spectra of 8-arm-PEG-MAES and 8-arm-PEG-A are shown in Fig. 2a and b, respectively. The acrylate proton peaks at 6.03, 6.22 and 6.43 ppm in both the NMR spectra of 8-arm-PEG-MAES and 8-arm-PEG-A confirmed the successful conjugation of MAES and AC to 8-arm-PEG.

In situ forming hydrogels were prepared by simply mixing two acrylate- and thiol-terminated PEG macromers in aqueous media at physiological pH. While M and A gels were composed of 8-arm-

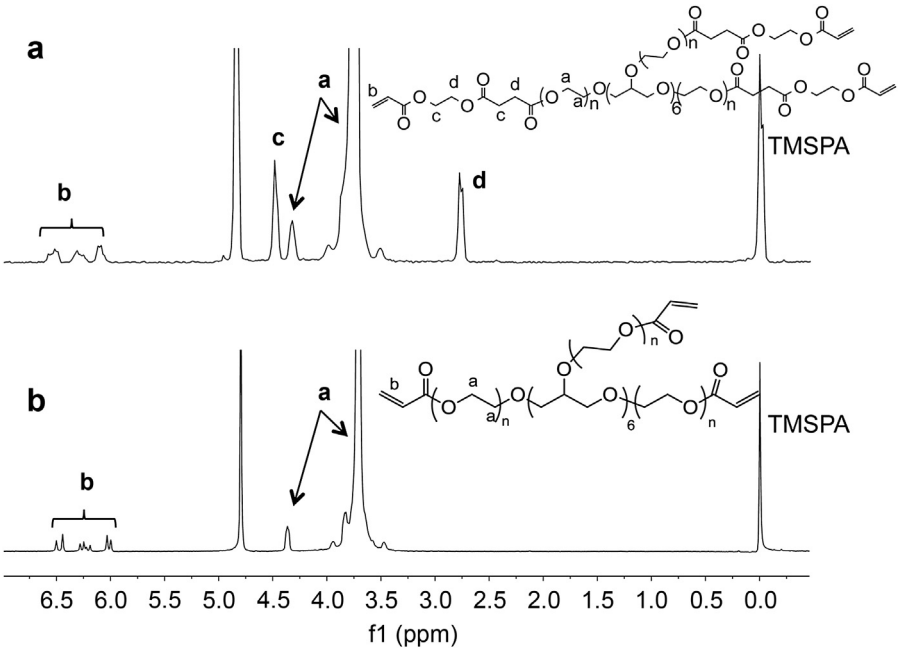

Fig. 2. ^{1}H NMR spectra of (a) 8-arm-PEG-MAES and (b) 8-arm-PEG-A.

PEG-MAES and 8-arm-PEG-A, respectively, with 8-arm-PEG-SH, MA gel was a mixture of 8-arm-PEG-MAES and 8-arm-PEG-A (weight ratio 2/1) with 8-arm-PEG-SH. Gelation rates of the hydrogels were observed via a tube inversion method [37] in PBS at pH 7.4. The M, MA and A gels were formed by 62.66 ± 2.51, 59.00 ± 3.60 and 53.00 ± 2.64 s, respectively, after mixing the acrylate and thiol PEG macromers.

3.2. Swelling kinetics, hydrogel degradation and rheology

Physical properties of the degradable hydrogels were examined through measurement of their swelling ratio changes, degradation profiles and rheological behavior. Hydrogel swelling and degradation increase polymer network pore size, thus accelerating the transport of oxygen and nutrients, and the removal of waste products from incorporated cells, and also providing space for new tissue formation [42–44]. Hence, controlling swelling ratio and degradation rate of hydrogels is important to regulate new tissue growth [42]. In addition, controlling these properties also permits loaded bioactive factors to be released in a tunable fashion [24,45]. Swelling and degradation of degradable hydrogels can be controlled by, for example, varying the degree of crosslinking [46], the molecular weight of crosslinkers [43,47], the macromer concentration [24,43] and the macromer molecular weight [44]. These physical properties in PEG hydrogel systems formed via Michael type reaction have been regulated by changing the hydrogel macromer concentration, degree of crosslinking [48], and macromer molecular weight [49] and the crosslinker molecular weight [43]. In this study, the swelling kinetics and degradation rates were tailored by tuning the density of degradable ester linkages in the hydrogel while maintaining a constant hydrogel macromer concentration.

All the gels reached equilibrium swelling after one day incubation in PBS (Fig. 3a). Swelling of the M gels remained relatively constant over one week, and then their swelling increased rapidly to a maximum at day 20. Compared to the M gels, swelling kinetics of the MA and A gels stayed relatively constant longer and reached maximum values at 31 and 55 days, respectively.

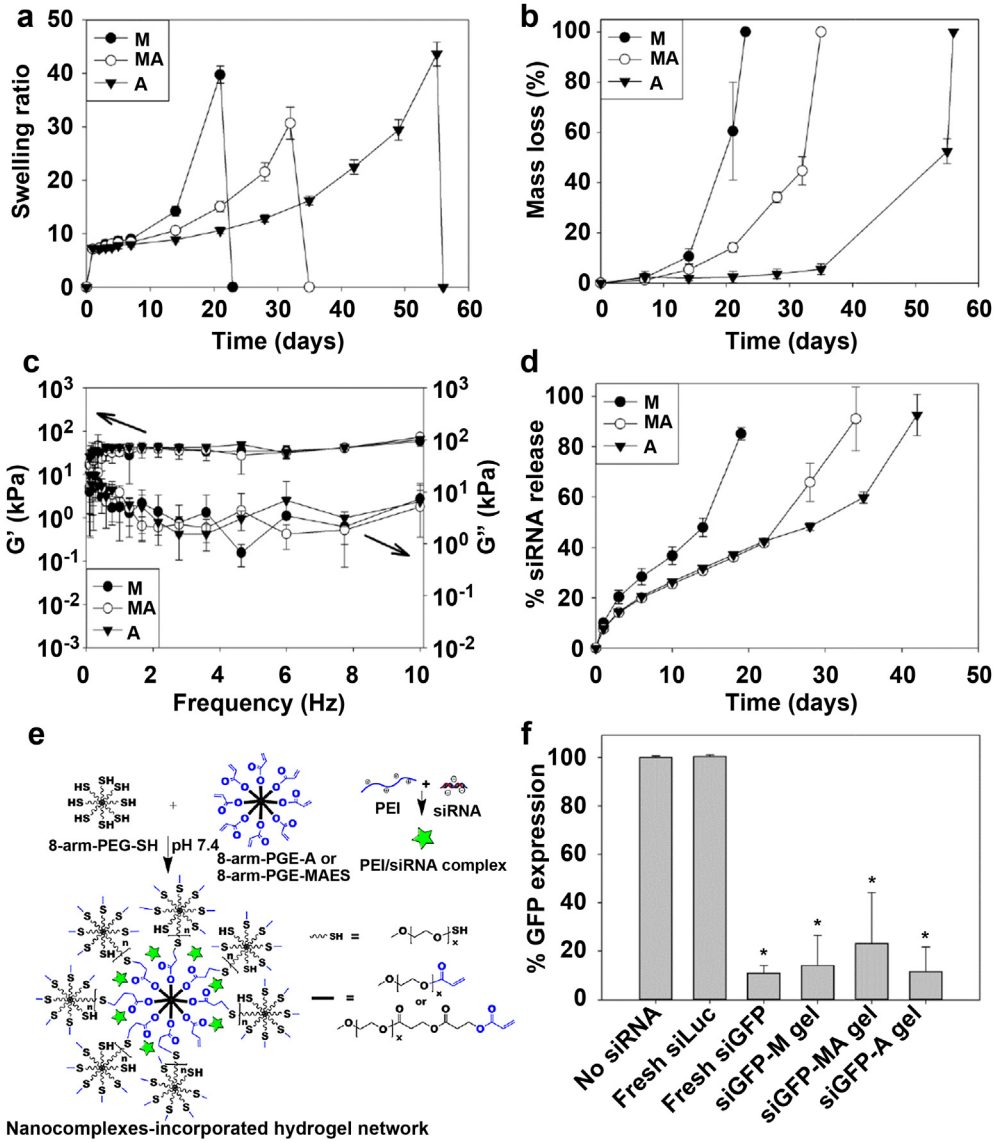

Fig. 3. a) Swelling, b) degradation profiles and c) rheological properties of the hydrogels. d) Release profiles of siRNA/PEI complexes from the hydrogels. e) Schematic figure of siRNA/PEI complex incorporation into the hydrogels. f) Bioactivity of siRNA/PEI released from M, MA and A gels compared to that of fresh siRNA/PEI complexes and no siRNA control. $^{*}p < 0.05$ compared with the no siRNA control group.

Hydrogel degradation was determined by measuring mass loss (%) of the hydrogels over time (Fig. 3b). The M gels degraded slowly for the first 2 weeks before their hydrolytic degradation kinetics increased rapidly achieving complete degradation by 3 week. Similarly, the MA gels initially degraded gradually, and then their degradation accelerated after 3 weeks and completely degraded by 34 days. Mass loss of the A gels was minimal for the first 5 weeks, and did not completely degrade until 8 weeks. There were three hydrolyzable ester groups on each arm of the 8-arm-PEG-MAES and one ester group on each arm of the 8-arm-PEG-A. Therefore, the faster degradation of the M gels was expected as a result of their higher ester density than the A and MA gels. These PEG materials presented *in vitro* hydrolytic degradation profiles from 3 to 8 weeks, which are substantially longer than previously reported *in situ* forming PEG hydrogels, which persisted for 7–23 days *in vitro* [43,48,49].

It was then determined whether the change in the chemical structure of the PEG acrylate macromers affected hydrogel mechanical properties. Mechanical response of the hydrogels was examined by measuring their rheological properties under oscillatory strain. Storage (G′) and loss moduli (G″), that represent the hydrogel elastic and viscous properties, respectively, of the M, MA and A gels are shown in Fig. 3c. G′ of the three hydrogel groups were similar and higher than G″, indicating the elasticity of the hydrogels was dominant in the whole range of tested frequencies (0.1–10 Hz).

3.3. siRNA release and bioactivity

It is challenging to have cells take up naked siRNA because it possesses anionic and macromolecular characteristics; therefore delivery carriers are usually required to facilitate cellular uptake before siRNA is released in the cytoplasm to perform its function [50]. PEI, a cationic polymer, has been used to bind siRNA and miRNA to form nanocomplexes that can effectively deliver siRNA to cells [51,52]. Therefore, siRNA/PEI complexes were incorporated into the three different hydrogel compositions and their release was measured over time (Fig. 3d). The complexes were prepared separately and homogeneously mixed with hydrogel macromers

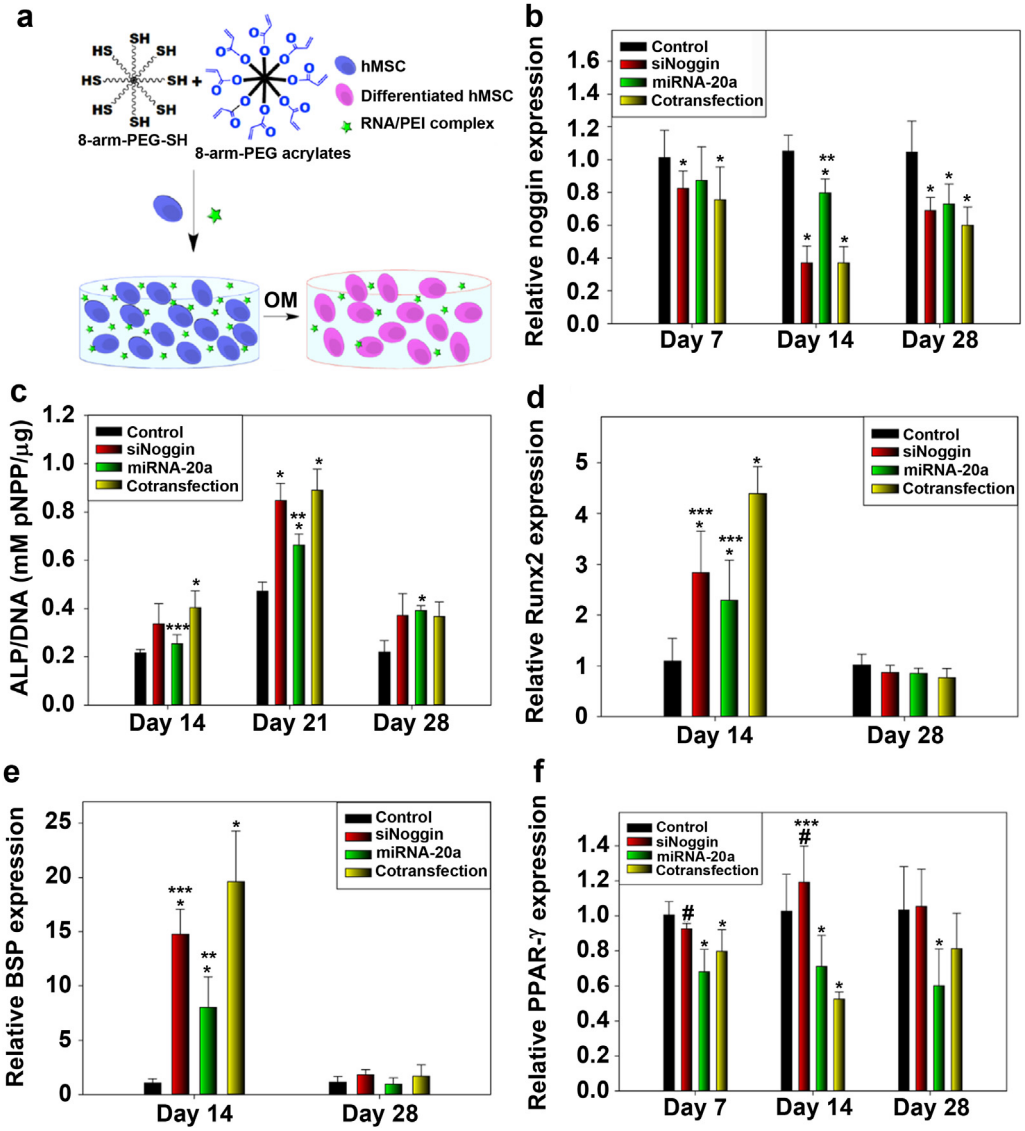

Fig. 4. a) Schematic figure depicting RNA and hMSCs encapsulation into the hydrogels and subsequent hMSC differentiation in osteogenic media (OM). b) Noggin gene expression, c) ALP activity, d) Runx2 gene expression, e) BSP gene expression and f) PPAR-γ gene expression of hMSCs encapsulated within the hydrogels. The expression of these genes was normalized to the control group at each time point. $^{*}p < 0.05$ compared with control, $^{**}p < 0.05$ compared with siNoggin and cotransfection, $^{***}p < 0.05$ compared with cotransfection, and $\#p < 0.05$ compared with miRNA-20a at specific time point.

prior to gelation for their incorporation (Fig. 3e). The release rate of complexes from the M gels was faster than that from the MA and A gels. While the M gels released 85.09 ± 2.43% siRNA over 19 days, the MA and A gels released 90.99 ± 12.67 and 92.57 ± 8.18% siRNA over 35 and 42 days, respectively. These results indicate that siRNA/PEI complexes were retained in the hydrogels and slowly released over a prolonged period of time. The rate of sustained delivery from each type of hydrogel was likely a function of the concentration of ester linkages in the macromolecular networks.

To confirm that the hydrogels can protect and preserve the bioactivity of siRNA over the entire release period, siGFP and siLuc, a non-targeting control, were complexed with PEI, and then the complexes were incorporated into the hydrogels. The siRNA/PEI complexes collected at the last time point prior to complete gel degradation were tested to assess their capability to silence GFP expression in HEK293 cells constitutively expressing deGFP. Cells were treated with equal amounts of the released siRNA/PEI or freshly prepared siRNA/PEI complexes. Percent GFP knockdown was normalized to the untreated cells in media only (controls), and compared to the freshly prepared siGFP and siLuc complexes. As shown in Fig. 3f, average GFP expression of the cells treated with the fresh or released siGFP/PEI was significantly reduced to 10.90–23.26% of the untreated control group. siLuc released from the hydrogels did not reduce GFP expression in comparison to the untreated control cell group (Fig. S3). These results indicate that the bioactivity of the released siRNA was preserved.

3.4. Osteogenic differentiation of encapsulated hMSCs

Having demonstrated that the hydrogel biomaterials could retain encapsulated siRNA over a prolonged period of time and that the released siRNA was still bioactive, the capacity of the system to actually regulate stem cell fate was then examined. We investigated whether the RNA/hydrogel constructs could drive a cellular process that would be valuable for regenerative medicine, such as osteogenic differentiation of hMSCs encapsulated in the hydrogels for bone tissue engineering. In the current study, siRNA against noggin (siNoggin) and miRNA-20a were delivered separately or in combination in a controlled, sustained manner from *in situ* forming PEG hydrogels (A gels) to determine if this approach could accelerate the osteogenic differentiation of encapsulated hMSCs (Fig. 4). After coencapsulation of siRNA and hMSCs into the hydrogels, viability of the hMSCs was assessed using a live/dead assay and remained high, as shown in Fig. S4, indicating the cytocompatibility of the system.

To evaluate noggin suppression in encapsulated hMSCs by siNoggin delivery from the *in situ* forming hydrogels, noggin mRNA expression was measured by qRT-PCR over the course of 4 weeks. Encapsulated hMSCs exhibited significant gene silencing of noggin at all time points measured within the 3D microenvironment by delivering siNoggin and codelivering siNoggin and miRNA-20a (cotransfection), as compared to the control group (i.e., hMSCs in gels with non-targeting negative control RNA) (Fig. 4b).

To investigate the effect of localized, sustained delivery of siNoggin and/or miRNA-20a on osteogenesis of encapsulated hMSCs, hMSC/hydrogel constructs were first evaluated for ALP activity, which is an important early marker for osteogenic differentiation (Fig. 4c). At day 14, ALP activity normalized to construct DNA content of the cotransfection group was significantly higher than that of the control and miRNA-20a groups. At day 21, all groups exhibited a peak ALP activity followed by a decrease by day 28. The ALP activity of hMSCs in the siNoggin, miRNA-20a, and cotransfection groups was significantly higher than that of control group at day 21. Since other cell phenotypes can produce ALP, it is important to examine additional, more specific, osteogenic differentiation markers as well. Therefore, quantitative analysis of mRNA expression levels of Runt-related transcription factor 2 (Runx2), which is one of the earlier and most specific osteogenic differentiation makers, and bone sialoprotein (BSP), which is a later osteogenic differentiation marker, were evaluated by qRT-PCR (Fig. 4d and e). Runx2 and BSP expression in the siNoggin, miRNA-20a, and cotransfection groups was significantly higher than that of the control group at day 14.

Since miRNA-20a can down-regulate the mRNA expression of peroxisome proliferator-activated receptor gamma (PPAR-γ) [12], which is an adipogenic transcription factor and a negative regulator of BMP-2 signaling in osteogenesis [53], its mRNA expression over time was evaluated by qRT-PCR to determine whether PPAR-γ was suppressed during the osteogenic differentiation of hMSCs by

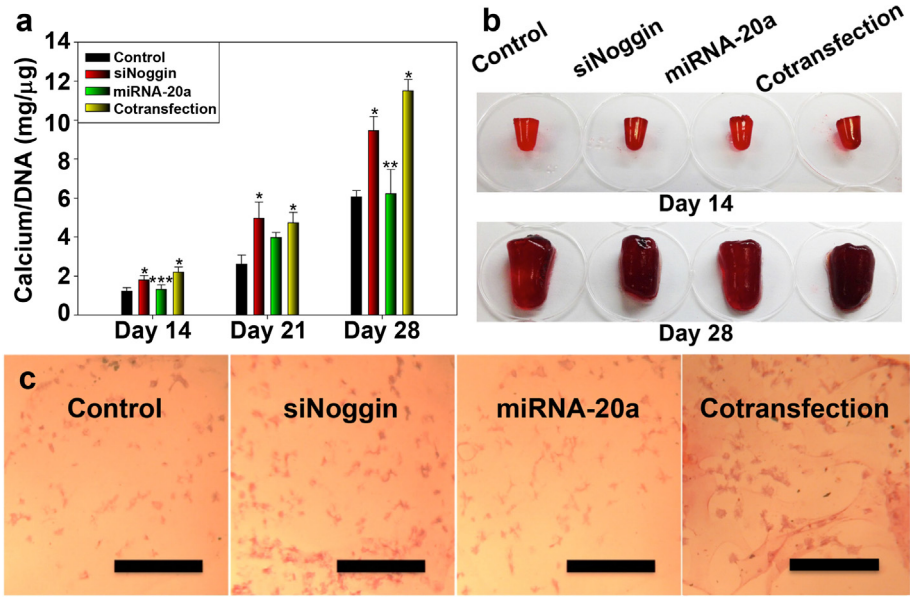

Fig. 5. a) Calcium content in hydrogels. $^{*}p < 0.05$ compared with control, $^{**}p < 0.05$ compared with siNoggin and cotransfection, and $^{***}p < 0.05$ compared with cotransfection at specific time point. All groups exhibited a significant ($p < 0.05$) increase in calcium content over time. Mineralization in b) bulk and c) sectioned (day 14) hydrogels stained with Alizarin red. The scale bars indicate 200 μm.

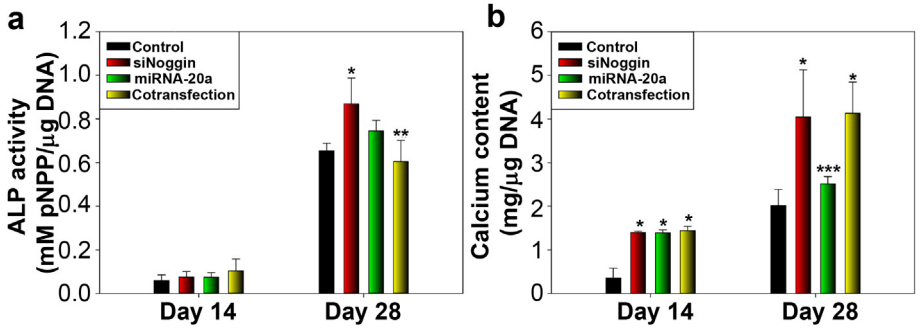

Fig. 6. a) ALP activity and b) calcium content in hMSC (2nd donor)-hydrogel constructs. $^{*}p < 0.05$ compared with control, $^{**}p < 0.05$ compared with siNoggin, and $^{***}p < 0.05$ compared with siNoggin and cotransfection at a specific time point.

sustained siNoggin and/or miRNA-20a presentation using the *in situ* forming PEG hydrogels. As exhibited in Fig. 4f, while siNoggin transfection did not significantly alter PPAR-γ expression compared to the control group, PPAR-γ expression of miRNA-20a and cotransfection groups was significantly lower than that of the control at days 7 and 14. Interestingly, PPAR-γ suppression was further sustained for 28 days in miRNA-20a group.

Since mineralization is the ultimate indicator of osteogenic differentiation, the calcium deposition in the hMSC/hydrogel constructs was evaluated by quantification of calcium content and Alizarin red staining. As shown in Fig. 5, calcium deposition normalized to construct DNA content significantly increased by transfection with siNoggin or cotransfection of siNoggin and miRNA-20a at days 14, 21 and 28 compared to the control (DNA content shown in Fig. S1). Calcium content of all groups increased over time since the hydrogels were cultured in osteogenic media. Similar to the calcium content results, siNoggin and cotransfection constructs stained more intensely for mineralization with Alizarin red than the other two conditions at these time points. Since the miRNA-20a group exhibited significantly higher ALP activity at day 21, and Runx2 and BSP gene expression at day 14 compared to control group, it was expected that calcium deposition would also be enhanced. However, unlike its effect on other osteogenic differentiation markers, miRNA-20a transfection appeared to have minimal effect on calcium deposition compared to the control group.

To verify that these results were not donor specific, the osteogenic differentiation study was repeated with hMSCs from a second donor. The ALP activity normalized to construct DNA content of siNoggin group was significantly higher than the control and cotransfection groups at day 28 (Fig. 6a). The calcium content normalized to construct DNA content in the siNoggin, miRNA-20a and cotransfection groups was significantly greater than the control at day 14, but only hMSCs in the siNoggin and cotransfection groups produced significantly higher calcium levels than the control group at day 28 (Fig. 6b; DNA content shown in Fig. S2).

4. Conclusion

In situ forming biodegradable and cytocompatible hydrogels were engineered for sustained and localized delivery of siRNA and miRNA for differentiation of encapsulated hMSCs. The biomaterial permitted homogeneous encapsulation of cells and RNA in mild gelling conditions without the need of UV light or a photoinitiator. The swelling and degradation properties of the *in situ* forming hydrogels were controlled via the density of hydrolyzable ester groups in the materials. While the gene inhibiting effect of exogenous transfection with siRNA or miRNA is usually transient, especially in rapidly dividing cells, prolonged delivery of siRNA and/or miRNA from this polymeric scaffold permitted extended regulation of cell behavior. *In situ* PEG hydrogels released the siRNAs in a sustained manner, and the siRNAs were shown to retain their bioactivity for up to 7 weeks. Importantly, the prolonged delivery of siNoggin or siNoggin/miRNA-20a using *in situ* forming PEG hydrogels enhanced the osteogenic differentiation of encapsulated hMSCs. This system may provide a promising platform for controlled and sustained delivery of siRNA and miRNA to regulate stem cell fate for a wide range of applications in tissue regeneration.

Acknowledgments

The authors gratefully acknowledge funding from the National Institute of Dental & Craniofacial Research of the National Institutes of Health (R56DE022376; EA), the Department of Defense Congressionally Directed Medical Research Programs (OR110196; EA) and a National Science Foundation Graduate Research Fellowship (MDK).

Appendix A. Supplementary data

Supplementary data related to this article can be found at http://dx.doi.org/10.1016/j.biomaterials.2014.04.048.

References

[1] Chen S, Do JT, Zhang Q, Yao S, Yan F, Peters EC, et al. Self-renewal of embryonic stem cells by a small molecule. Proc Natl Acad Sci U S A 2006;103:17266–71.
[2] Jaiswal RK, Jaiswal N, Bruder SP, Mbalaviele G, Marshak DR, Pittenger MF. Adult human mesenchymal stem cell differentiation to the osteogenic or adipogenic lineage is regulated by mitogen-activated protein kinase. J Bio Chem 2000;275:9645–52.
[3] Kwong F, Richardson S, Evans C. Chordin knockdown enhances the osteogenic differentiation of human mesenchymal stem cells. Arthritis Res Ther 2008;10:R65.
[4] Tzeng SY, Hung BP, Grayson WL, Green JJ. Cystamine-terminated poly(beta-amino ester)s for siRNA delivery to human mesenchymal stem cells and enhancement of osteogenic differentiation. Biomaterials 2012;33:8142–51.
[5] Ramasubramanian A, Shiigi S, Lee G, Yang F. Non-viral delivery of inductive and suppressive genes to adipose-derived stem cells for osteogenic differentiation. Pharm Res 2011;28:1328–37.
[6] Zimmerman LB, De Jesús-Escobar JM, Harland RM. The spemann organizer signal noggin binds and inactivates bone morphogenetic protein 4. Cell 1996;86:599–606.
[7] Aspenberg P, Jeppsson C, Economides A. The bone morphogenetic proteins antagonist noggin inhibits membranous ossification. J Bone Min Res 2001;16:497–500.
[8] Devlin RD, Du Z, Pereira RC, Kimble RB, Economides AN, Jorgetti V, et al. Skeletal overexpression of noggin results in osteopenia and reduced bone formation. Endocrinology 2003;144:1972–8.
[9] Wu XB, Li Y, Schneider A, Yu W, Rajendren G, Iqbal J, et al. Impaired osteoblastic differentiation, reduced bone formation, and severe osteoporosis in noggin-overexpressing mice. J Clin Invest 2003;112:924–34.

[10] Wan DC, Pomerantz JH, Brunet LJ, Kim J-B, Chou Y-F, Wu BM, et al. Noggin suppression enhances in vitro osteogenesis and accelerates in vivo bone formation. J Biol Chem 2007;282:26450–9.
[11] Eskildsen T, Taipaleenmäki H, Stenvang J, Abdallah BM, Ditzel N, Nossent AY, et al. MicroRNA-138 regulates osteogenic differentiation of human stromal (mesenchymal) stem cells in vivo. Proc Natl Acad Sci U S A 2011;108:6139–44.
[12] Zhang J-F, Fu W-M, He M-L, Xie W-D, Lv Q, Wan G, et al. MiRNA-20a promotes osteogenic differentiation of human mesenchymal stem cells by co-regulating BMP signaling. RNA Biol 2011;8:829–38.
[13] Geckil H, Xu F, Zhang X, Moon S, Demirci U. Engineering hydrogels as extracellular matrix mimics. Nanomedicine 2010;5:469–84.
[14] Krebs MD, Alsberg E. Localized, targeted, and sustained siRNA delivery. Chem Eur J 2011;17:3054–62.
[15] Krebs MD, Jeon O, Alsberg E. Localized and sustained delivery of silencing RNA from macroscopic biopolymer hydrogels. J Am Chem Soc 2009;131:9204–6.
[16] Cao H, Jiang X, Chai C, Chew SY. RNA interference by nanofiber-based siRNA delivery system. J Control Release 2010;144:203–12.
[17] Rujitanaroj P-O, Wang Y-C, Wang J, Chew SY. Nanofiber-mediated controlled release of siRNA complexes for long term gene-silencing applications. Biomaterials 2011;32:5915–23.
[18] Chen M, Gao S, Dong M, Song J, Yang C, Howard KA, et al. Chitosan/siRNA nanoparticles encapsulated in PLGA nanofibers for siRNA delivery. ACS Nano 2012;6:4835–44.
[19] Nelson CE, Gupta MK, Adolph EJ, Shannon JM, Guelcher SA, Duvall CL. Sustained local delivery of siRNA from an injectable scaffold. Biomaterials 2012;33:1154–61.
[20] Han HD, Mora EM, Roh JW, Nishimura M, Lee SJ, Stone RL, et al. Chitosan hydrogel for localized gene silencing. Cancer Biol Ther 2011;11:839–45.
[21] Kim Y-M, Park M-R, Song S-C. Injectable polyplex hydrogel for localized and long-term delivery of siRNA. ACS Nano 2012;6:5757–66.
[22] Takahashi H, Wang Y, Grainger DW. Device-based local delivery of siRNA against mammalian target of rapamycin (mTOR) in a murine subcutaneous implant model to inhibit fibrous encapsulation. J Control Release 2010;147:400–7.
[23] Manaka T, Suzuki A, Takayama K, Imai Y, Nakamura H, Takaoka K. Local delivery of siRNA using a biodegradable polymer application to enhance BMP-induced bone formation. Biomaterials 2011;32:9642–8.
[24] Nguyen K, Dang PN, Alsberg E. Functionalized, biodegradable hydrogels for control over sustained and localized siRNA delivery to incorporated and surrounding cells. Acta Biomater 2013;9:4487–95.
[25] Jeon O, Powell C, Solorio LD, Krebs MD, Alsberg E. Affinity-based growth factor delivery using biodegradable, photocrosslinked heparin-alginate hydrogels. J Control Release 2011;154:258–66.
[26] Nguyen MK, Lee DS. Injectable biodegradable hydrogels. Macromol Biosci 2010;10:563–79.
[27] Slaughter BV, Khurshid SS, Fisher OZ, Khademhosseini A, Peppas NA. Hydrogels in regenerative medicine. Adv Mater 2009;21:3307–29.
[28] Bhakta G, Rai B, Lim ZXH, Hui JH, Stein GS, van Wijnen AJ, et al. Hyaluronic acid-based hydrogels functionalized with heparin that support controlled release of bioactive BMP-2. Biomaterials 2012;33:6113–22.
[29] Kinard L, Chu C-Y, Tabata Y, Kasper FK, Mikos A. Bone morphogenetic protein-2 release from composite hydrogels of oligo(poly(ethylene glycol) fumarate) and gelatin. Pharm Res 2013;30:2332–43.
[30] Vo TN, Kasper FK, Mikos AG. Strategies for controlled delivery of growth factors and cells for bone regeneration. Adv Drug Deliv Rev 2012;64:1292–309.
[31] Krebs MD, Salter E, Chen E, Sutter KA, Alsberg E. Calcium phosphate-DNA nanoparticle gene delivery from alginate hydrogels induces in vivo osteogenesis. J Biomed Mater Res Part A 2010;92A:1131–8.
[32] Chew SA, Kretlow JD, Spicer PP, Edwards AW, Baggett LS, Tabata Y, et al. Delivery of plasmid DNA encoding bone morphogenetic protein-2 with a biodegradable branched polycationic polymer in a critical-size rat cranial defect model. Tissue Eng Part A 2010;17:751–63.
[33] Huang YC, Simmons C, Kaigler D, Rice KG, Mooney DJ. Bone regeneration in a rat cranial defect with delivery of PEI-condensed plasmid DNA encoding for bone morphogenetic protein-4 (BMP-4). Gene Ther 2005;12:418–26.
[34] Mehta M, Schmidt-Bleek K, Duda GN, Mooney DJ. Biomaterial delivery of morphogens to mimic the natural healing cascade in bone. Adv Drug Deliv Rev 2012;64:1257–76.
[35] Mairhofer J, Grabherr R. Rational vector design for efficient non-viral gene delivery: challenges facing the use of plasmid DNA. Mol Biotechnol 2008;39:97–104.
[36] Elsabahy M, Nazarali A, Foldvari M. Non-viral nucleic acid delivery: key challenges and future directions. Curr Drug Deliv 2011;8:235–44.
[37] Vanderhooft JL, Mann BK, Prestwich GD. Synthesis and characterization of novel thiol-reactive poly(ethylene glycol) cross-linkers for extracellular-matrix-mimetic biomaterials. Biomacromolecules 2007;8:2883–9.
[38] Haynesworth SE, Goshima J, Goldberg VM, Caplan AI. Characterization of cells with osteogenic potential from human marrow. Bone 1992;13:81–8.
[39] Lennon D, Haynesworth S, Bruder S, Jaiswal N, Caplan A. Human and animal mesenchymal progenitor cells from bone marrow: identification of serum for optimal selection and proliferation. Vitro Cell Dev Biol Anim 1996;32:602–11.
[40] Nguyen MK, Huynh CT, Lee DS. pH-sensitive and bioadhesive poly(β-amino ester)–poly(ethylene glycol)–poly(β-amino ester) triblock copolymer hydrogels with potential for drug delivery in oral mucosal surfaces. Polymer 2009;50:5205–10.
[41] Sawhney AS, Pathak CP, Hubbell JA. Bioerodible hydrogels based on photopolymerized poly(ethylene glycol)-co-poly(.alpha.-hydroxy acid) diacrylate macromers. Macromolecules 1993;26:581–7.
[42] Drury JL, Mooney DJ. Hydrogels for tissue engineering: scaffold design variables and applications. Biomaterials 2003;24:4337–51.
[43] Zustiak SP, Leach JB. Hydrolytically degradable poly(ethylene glycol) hydrogel scaffolds with tunable degradation and mechanical properties. Biomacromolecules 2010;11:1348–57.
[44] Alsberg E, Kong HJ, Hirano Y, Smith MK, Albeiruti A, Mooney DJ. Regulating bone formation via controlled scaffold degradation. J Dent Res 2003;82:903–8.
[45] Garripelli VK, Kim JK, Namgung R, Kim WJ, Repka MA, Jo S. A novel thermosensitive polymer with pH-dependent degradation for drug delivery. Acta Biomater 2010;6:477–85.
[46] Jeon O, Bouhadir KH, Mansour JM, Alsberg E. Photocrosslinked alginate hydrogels with tunable biodegradation rates and mechanical properties. Biomaterials 2009;30:2724–34.
[47] Kong HJ, Alsberg E, Kaigler D, Lee KY, Mooney DJ. Controlling degradation of hydrogels via the size of crosslinked junctions. Adv Mater 2004;16:1917–21.
[48] Elbert DL, Pratt AB, Lutolf MP, Halstenberg S, Hubbell JA. Protein delivery from materials formed by self-selective conjugate addition reactions. J Control Release 2001;76:11–25.
[49] van de Wetering P, Metters AT, Schoenmakers RG, Hubbell JA. Poly(ethylene glycol) hydrogels formed by conjugate addition with controllable swelling, degradation, and release of pharmaceutically active proteins. J Control Release 2005;102:619–27.
[50] Gao K, Huang L. Nonviral methods for siRNA delivery. Mol Pharm 2008;6:651–8.
[51] Höbel S, Aigner A. Polyethylenimine (PEI)/siRNA-mediated gene knockdown in vitro and in vivo. In: Min W-P, Ichim T, editors. RNA Interference. Humana Press; 2010. pp. 283–97.
[52] Ibrahim AF, Weirauch U, Thomas M, Grünweller A, Hartmann RK, Aigner A. microRNA replacement therapy for miR-145 and miR-33a is efficacious in a model of colon carcinoma. Cancer Res 2011;71:5214–24.
[53] Lin TH, Yang RS, Tang CH, Lin CP, Fu WM. PPARgamma inhibits osteogenesis via the down-regulation of the expression of COX-2 and iNOS in rats. Bone 2007;41:562–74.